Results in Physics 13 (2019) 102171

Contents lists available at ScienceDirect

Results in Physics

journal homepage: www.elsevier.com/locate/rinp

Charge transport and electron recombination suppression in dye-sensitized solar cells using graphene quantum dots

N. Fadzilah M. Sharif[a,e,*], M.Z.A.A. Kadir[c,d], Suhaidi Shafie[a,b], Suraya Abdul Rashid[b], W.Z. Wan Hasan[a], Suraya Shaban[b]

[a] Department of Electrical and Electronics Engineering, Faculty of Engineering, Universiti Putra Malaysia, 43400 UPM Serdang, Selangor, Malaysia
[b] Institute of Advanced Technology, Universiti Putra Malaysia, 43400 UPM Serdang, Selangor Darul Ehsan, Malaysia
[c] Centre for Electromagnetic & Lightning Protection (CELP), Universiti Putra Malaysia, 43400 UPM Serdang, Selangor, Malaysia
[d] Institute of Power Engineering (IPE), Universiti Tenaga Nasional, Kuala Lumpur 57000, Malaysia
[e] Department of Electrical and Electronics Engineering, Faculty of Engineering, UPNM, Kuala Lumpur 57000, Malaysia

ARTICLE INFO

Keywords:
TiO_2-GQDs
Charge transport
Charge collection efficiency
GQDs-DSSC

ABSTRACT

In this study, TiO_2 photoelectrodes were sensitized in different concentration of Graphene Quantum Dots (GQDs) solution to enhance photovoltaic performance and charge transport of DSSC. The performance of pristine TiO_2 and TiO_2-GQDs photoelectrodes were compared to investigate the effect of GQDs incorporation in DSSC. It was found GQDs increased light absorption of TiO_2 photoelectrode at visible spectrum in the range of $\lambda = 375$ nm to $\lambda = 600$ nm, resulting highest current–density, Jsc and photon-to-current conversion efficiency, ηc. Solar cell sensitized in 7.5 mg/ml concentration of GQDs known as (PG 7.5) cell shown the highest reading by 15.49 mA cm^{-2} and 6.97%, which indicated an improvement by 28.07% and 70.83% for Jsc and η compare to pristine TiO_2 DSSC at 12.10 mA cm^{-2} and 4.08%. Photoluminescence property own by GQDs may enhance photon emission to visible region when uv-ray excited on solar cell. Thus, generate more electron-hole pairs in the photoelectrode and enhance the photovoltaic parameters of DSSC. PG 7.5 cell also exhibited lowest series resistance (Rs) of 36.60 Ω, highest charge transfer resistance (Rct2) of 41.98 Ω and electron lifetime of 6.33 ms among other DSSC. These possibly due to suppression of recombination between TiO_2/dye/electrolyte interfaces. Hence, resulting highest charge collection efficiency (CCE) of 53.42%. The EIS analysis confirmed the PV performance of the best cell of PG 7.5 since the same cell also generated the best photon-current conversion efficiency (PCE). This study revealed GQDs can enhanced photovoltaic parameter and charge collection efficiency of DSSC.

Introduction

DSSC is a type of photochemical cell which able to convert solar to electrical energy in moderate photon conversion efficiency (PCE). DSSC also offer other advantages such as easy fabrication, low cost and work under low light condition compare to first and second generation solar cells. In the past 20 years, the efficiency of DSSC has shown improvement with confirmed record of 14.1% achieved by Gratzel and teams at École Polytechnique Fédérale de Lausanne (EPFL) [1–3]. Hence, a research on DSSC elements such as near infrared (NIR) and natural dye-sensitizer [4–7], non-volatile polymer electrolyte [8], graphene counter electrode [9–11], glass frit assisted laser to seal DSSC [12] and modification of TiO_2 photoelectrode are crucial to improve PCE of DSSC. Work involved in TiO_2 photoelectrode modification including incorporation of metal nanoparticle for surface plasmon resonance effect, doping to tune energy band structure, growing graphene layer between FTO and TiO_2, and the use of graphene type nanomaterial in photoelectrode to enhance PCE of DSSC [13–17]. Literatures of [18–21] suggested graphene shown potential material for enhancing properties of DSSC. Thus, graphene known as 2-dimensional carbon atom has shown potential due to high optical transmittance (~98%), good conductivity and large theoretical specific surface area (2630 $m^2 g^{-1}$) where it suits to engineer the TiO_2 layer in DSSCs. Graphene also can be downsized by bottom-up technique using organic precursor to modify graphene band gap producing zero-dimensional Graphene Quantum Dots (GQDs).

Furthermore, Rung Long used GQDs material to modify TiO_2 surface which narrow the TiO_2-GQDs bandgap compare to pristine TiO_2,

* Corresponding author.
E-mail address: gs45158@student.upm.edu.my (N.F. M. Sharif).

https://doi.org/10.1016/j.rinp.2019.102171
Received 26 November 2018; Received in revised form 24 February 2019; Accepted 4 March 2019
Available online 05 March 2019

resulting higher photocatalyitic and photovotaic (PV) performance due to better charge separation. [22]. In addition, GQDs was incorporated in DSSC to overcome the drawback of TiO_2 such as high carrier recombination, lack of charge-carrier transport and poor absorption on visible-region [23,24]. Xiaoli et al proved the composite GQDs-TiO_2 enhanced photo current density and efficiency by 30.9% and 19.6% respectively compare to pure TiO_2 photoelectrode [25]. Wang et al reported that the GQDs also used to tune the bandgap energy of semiconducting layer TiO_2 due to quantum confinement effect. Hence the absorption edge expands to visible region spectrum. A doping GQDs-TiO_2 mixture improved the photocatalytic activity resulted in higher visible light absorption which can be applied in light harvesting application. Pan et al fabricated photoelectrode based GQDs sensitized TiO_2 for stable photoelectrochemical device [26,27].

Therefore, based on previous study, it shown that GQDs properties help to expand the light absorption to visible region, improve charge transport and performance of DSSC. However, there is less attention on the effect of GQDs concentration in charge transport and charge collection efficiency enhancement in DSSC. Thus, in this study, GQDs concentration was varied to improve photovoltaic performance and charge collection efficiency of DSSC. The TiO_2 photoelectrode was sensitized in different concentration of GQDs then continue with dye-adsorption process. The performance of cell incorporated GQDs were compared to pristine TiO_2 cell.

Experimental details

Material

Titania powder of < 29 nm and FTO glass were purchased from Sigma Aldrich. N-719 dye, Iodolyte AN-50 solvent-based electrolyte and polymer spacer of 25 μm was obtained from Solaronix Switzerland. Platinum solution for counter electrode consist of isopropyl alcohol (IPA) and hexachloroplanitic acid hexahydrate was prepared in our lab. Commercial biochar from palm oil agrowaste received and subject to ball-milling for 24 h to produce nanosize carbon powder. Other chemical such as acetone and ethanol were obtained from Merck and used without further purification.

Methods

GQDs synthesis process

Firstly, a biochar powder and solvent were mixed in small size of stainless-steel reactor. Then the mixture was shake well. Argon gas was flown into mixture and the reactor capped was tightened. After that, the reactor was subjected to sonication process for 5 min. The reactor was then placed in the oven for thermal process at 250 °C for 1 h to exfoliate the biochar. After cooled at room temperature, the mixture was centrifuged at 4000 rpm to separate liquid and solid phase. A liquid phase consists of GQDs with ~5 nm in size was produced. No acid or harsh chemical were used during the synthesis process. However, to study the impact of GQDs on photoelectrode, the concentration of GQDs will be varied from 2.5, 5, 7.5 and 10 mg/ml using same solvent as synthesis process. Hence, the modified photoelectrodes with GQDs incorporation namely as PG 2.5, PG 5.0, PG 7.5 and PG 10 respectively. However, pristine TiO_2 photoelectrode known as PT. The performance of pristine TiO_2 and modified TiO_2-GQDs cells will be measured and studied.

TiO_2 paste preparation

Initially, solution A consisting of 6 g of TiO_2 powder with 0.5 ml acetic acid and DI water was ground for 5 min. Then 21 ml of ethanol was added and continued the grinding for 20 min. Next, 100 ml ethanol was added to the mixture. The mixture was sonicated for 1 h to disperse the nanoparticles. Another mixture called solution B, which consisted of 38 ml ethanol and 3 g of ethyl cellulose, was stirred for 2 h to form a binder solution. Then both solution A and B were stirred for 12 h and both mixtures evaporated to reach about 1/10th the size from the initial volume

DSSC fabrication

For photoelectrode fabrication, a Fluorine doped tin oxide coated glass slide (FTO) with active area of 1 cm^2 was prepared by screen-printing technique using TiO_2 paste. The thickness of TiO_2 layer produced was ~10 μm. Then the film was sintered at 450 °C for 30 min. The film was cooled at 80 °C before sensitizing with different concentration of GQDs. This method was modified from reference [25], where this work differ on GQDs synthesis process and additional of titanium tetrachloride ($TiCl_4$) treatment on photoelectrode fabrication. At this stage, different configuration photoelectrodes were fabricated where the performance of solar cell with TiO_2-GQDs and pristine TiO_2 parameters such as short-circuit current, open-circuit voltage, fill factor and efficiency values will be compared. Also, pre- and post- $TiCl_4$ treatments were carried out to enhance conductivity of photoelectrode in DSSC. Then continue with dye adsorption using N-719 and ethanol was used to clean the thin film to remove any loose dye particle. However, other set-up parameters of the cells such as amount electrolyte, dye molarity and dye loading time were constant. To make a complete cell of DSSC, an electrolyte was dropped between FTO glass of photoelectrode and counter electrode which were attached with platinum electrode by 25 μm polymer spacer to form a sandwich structure of solar cell. A complete DSSC fabrication process is shown in Fig. 1.

Characteristic

GQD and photoelectrode characteristic

In this study, the GQDs size detail was measured using high-resolution transmission electron microscopy (HRTEM, FEI Tecnai G2 F20, 200 kV, Thermo Fisher Scientific, USA). The photoluminescence (PL) emission of GQD was measured using LS 55 luminescence spectroscopy of PerkinElmer Ltd. UK at ambient temperature using xenon lamp of 20 kW. The EDX was done using FESEM (FEI, NovaNanoSem230, Holland) to obtain the existence of GQD after sensitizing process. Ultraviolet spectroscopy (Uv–vis) of (Lambda 25, PerkinElmer, USA) was used to determine the absorption intensity after GQD and N-719 incorporation. Current-voltage performance of complete DSSC was obtained using Keithley 2601 solar simulator under illumination using an AM 1.5 simulated light with an intensity of 100 mW cm^{-2}. Finally, the electrochemical study was measured using Autolab PGSTAT 204.

EIS measurement

The photovoltaic performance of DSSC such as short-circuit current density, open-circuit voltage and photon current conversion efficiency can be obtained from IV-measurement. However, the photoelectrochemical behavior of DSSCs such as series and charge-transfer resistance, electron lifetime and charge collection efficiency can only be obtained using electrochemical impedance spectroscopy (EIS). The EIS measurements using Autolab PGSTAT 204 was carried out in a frequency range between 0.01 Hz and 100 kHz to study the interfacial charge transfer process of DSSC as explain in Eqs. (1)–(4). The Nyquist and bode plots will generated from EIS measurement to show the sheet, charge-transfer resistance and angular frequency for DSSC measured. Ƭn is electron lifetime and can be obtained from Eq. (1), where ω_{max} is maximum frequency obtained from bode plot.

$$\tau_n = \frac{1}{2\pi f} \quad (1)$$

Using τ_n and R_{ct} value from the Nyquist plot, electrochemical

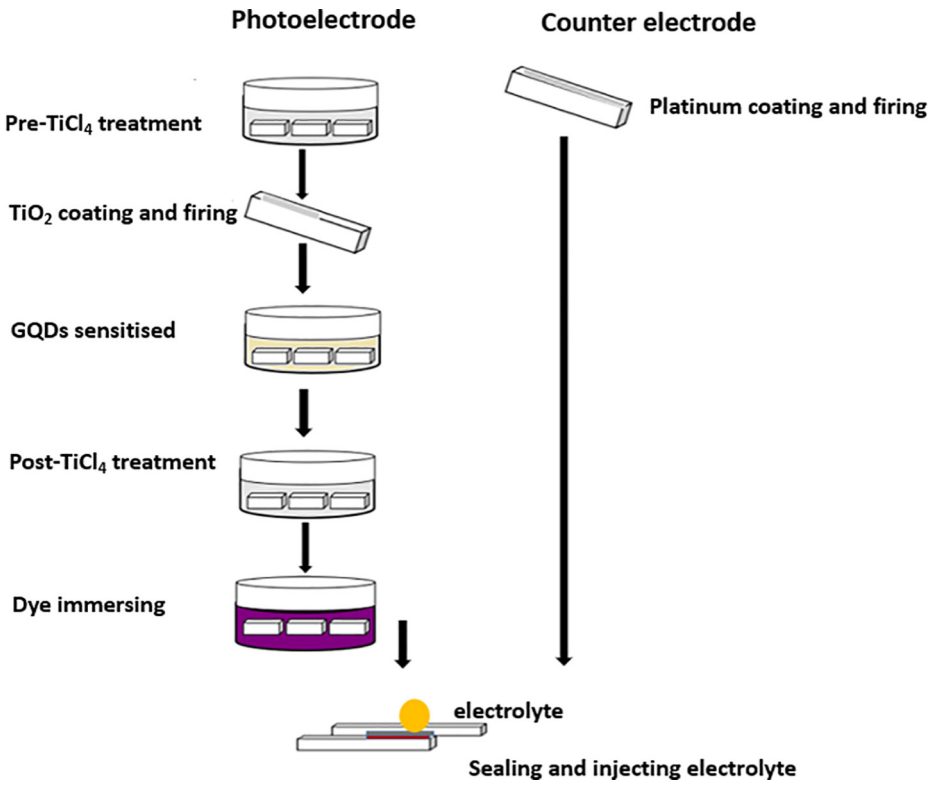

Fig. 1. DSSC fabrication process.

capacitance was calculated from the Eq. (2) below.

$$\tau_n = R_{ct} C_u \quad (2)$$

Hence, the electron transport time τ_s is given in Eq. (3)

$$\tau_s = R_s C_u \quad (3)$$

Finally, the charge collection efficiency η_c is calculated as Eq. (4).

$$\eta_c = (1 + R_s/R_{ct})^{-1} \quad (4)$$

Results and discussion

GQDs properties

A GQDs physical and its PL properties used to improve DSSC performance in this study are discussed in this section. Fig. 2(a) shown TEM image of as-prepared GQDs solution which shown non-uniform size of carbon dots. Fig. 2(b) depicted the structure of GQDs which showing single GQD particle with layer spacing of 0.25 nm, which is similar to work reported by [28,29] and Fig. 2(c) shown a size distribution of GQDs where the red line is the Gaussian fitting curve to estimate size distribution of GQDs at 5 nm. The Photoluminescence spectra of GQDs in this study is shown in Fig. 3, where GQDs generated upconverted emission PL spectra from 459 to 473 nm when excited with 365 to 400 nm wavelength. Hence the GQD produced in this work are having stokes-shift phenomenon, where the PL emission of a substance is at a higher wavelength than the light used to excite the substance. This property is vital, since it can improve light absorption in the photoelectrode. Hence enhance the current density and photon-current conversion efficiency. Inset image in Fig. 3 shown GQDs solution under ambient light on the left side and blue greenish PL shown GQD solution under uv-light on the right side.

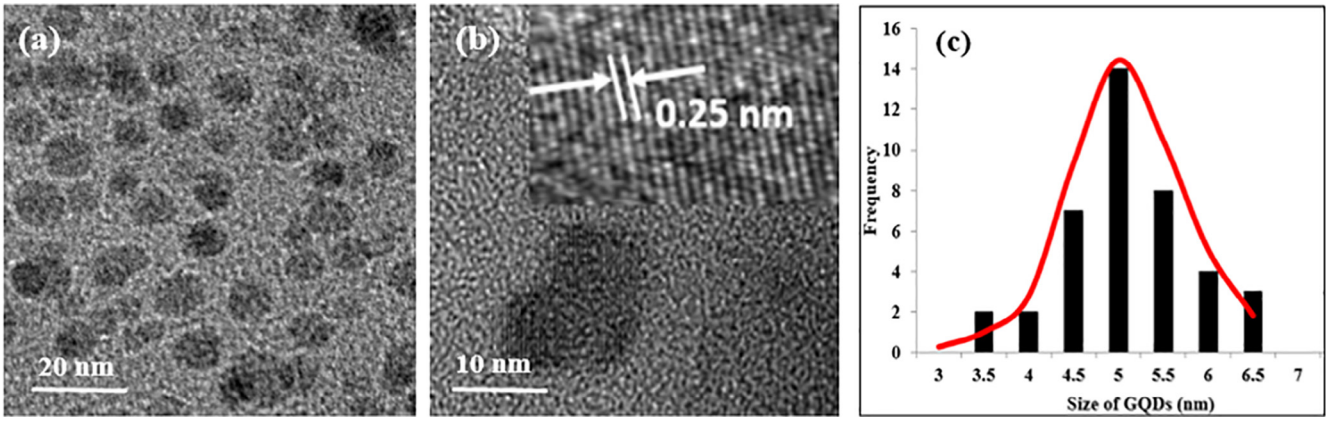

Fig. 2. (a) TEM image of GQDs solution (b) TEM image of single GQD particle with inset picture shown lattice spacing of GQDs with 0.25 nm (c) Size distribution of GQDs where the red line is the Gaussian fitting curve. (For interpretation of the references to colour in this figure legend, the reader is referred to the web version of this article.)

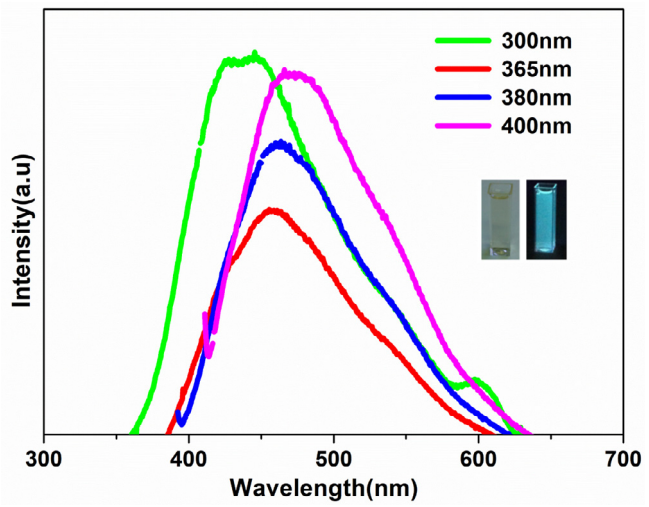

Fig. 3. Upconverted photoluminescence (PL) spectra of the graphene quantum dots (GQDs) at different excitation wavelengths. The inset picture represented GQD solution under ambient light (left) and GQD under uv-light (right).

Absorption spectra of pristine TiO_2 and modified TiO_2-GQDs photoelectrode

In this section, Fig. 4(a) represented the absorption spectra of GQDs solution at different GQDs content at the 290 nm wavelength. GQDs at 7.5 mg/ml produced higher absorption intensity, followed by 5.0, 2.5 and finally 10 mg/ml solution. Inset image in Fig. 4(a) shown, the TiO_2–GQDs photoelectrode was looked yellowish (right side) compare to pristine TiO_2 photoelectrode (left side), which indicate the GQDs adsorbed onto TiO_2 surface after soaking process. The photoanode appearance of TiO_2–GQDs films were similar to work by Wang et al. [30], where similar method was applied to incorporate GQDs onto TiO_2 film. Then, the absorption spectra of TiO_2 and TiO_2 – GQDs films were measured using Uv–Vis to see the enhancement of light absorption after the photoelectrode was sensitized with GQDs solution. The absorption spectra of cells PT and modified photoelectrode of PG 2.5, 5.0, 7.5 and 10 after sensitising GQDs and dye-N719 are shown in Fig. 4(b) and (c) respectively, where the absorption intensity of PG 7.5 was the highest compare to other photoelectrode in the range of $\lambda = 375$ nm to $\lambda = 600$ nm.This obviously shown after incorporation of GQDs in TiO_2 photoelectrode the light absorption was stronger in the ultraviolet and slightly enhanced in the visible-light region. Therefore, this phenomenon will enhance the short- circuit current and photon-current efficiency of DSSC [31].

Field emission scanning electron microscopy (FESEM) analysis

Fig. 5(a–d) shown the surface and cross sectional SEM images of pristine TiO_2 and TiO_2-GQDs films to study the morphology of films. Surface image in Fig. 5(b) shown, the pores of spongy-like TiO_2-GQDs films slightly bigger after GQDs sensitized. However, cross-sectional image shown not much different after GQDs sensitized on TiO_2 film due to GQDs nano-size in Fig. 5(c) and (d). EDX study was carried out to determine elements in both pristine TiO_2 and the PT 2.5 films, where Fig. 6 shown (a) pristine TiO_2 film which consist of wt% of 56.83% titanium and 43.17% oxygen. Fig. 6(b), on the other hand shown the best photoelectrode of PG 2.5 film consist of wt% of Titanium (Ti), oxygen (O) and carbon (C) elements by 58.27%, 40.58% and 1.15% respectively. It is proven the carbon element from graphene family of GQD existed in photoelectrode of DSSC [32].

Photovoltaic measurement

The photovoltaic parameters for both TiO_2 and modified TiO_2-GQD DSSC are summarized in Table 1 and the J-V curves of DSSC are presented in Fig. 7. As seen in Table 1, the current density, Jsc value was 12.10 mA/cm^2 then decreased for PG 2.5 and PG 5.0. Then the Jsc was increased for cell PG 7.5 and finally decreased at for PG 10 cell. The Jsc and photon conversion efficiency, η of cell sensitized in 7.5 mg/ml concentration of GQDs known as (PG 7.5) cell shown the highest performance by 28.07% and 70.83% compare to PT cell. This possibly due to PL property own by GQDs which it can enhance photon emission to visible region when uv-ray excited on solar cells [18–21]. Thus, it will generate more electron-hole pairs in the photoelectrode and enhance the photovoltaic parameters of Jsc and η of DSSC. The Jsc enhancement in PG 7.5 cell relevant to the improvement of light absorption measured by UV–vis as represented in Fig. 4(b) and (c). The open-circuit voltage of all cells generally equal to 0.75 v may due to constant potential different between electrolyte and dye sensitizer. The fill factors generated for all TiO_2-GQD cells are higher compare to pristine TiO_2 cell except for cell of PG 10. As the GQDs concentration get higher in PG 10, the amount of QDs also increased at 10 mg/ml. Hence, aggregations were easily happened between the graphene dots due to great molecular attraction within the solution and formed larger size of graphene molecule on photoanode surface [24,25,33]. As a result, the agglomeration of GQDs in 10 mg/ml may decreased the photon to current conversion efficiency of PG 10 at 4.75% and generate lowest fill factor among cell at 0.45 as shown in Table 1, which affecting its performance [36]. However, cells of PG 2.5, 5.0 and 7.5 Cells were generated fill factors of ~0.60–0.66.

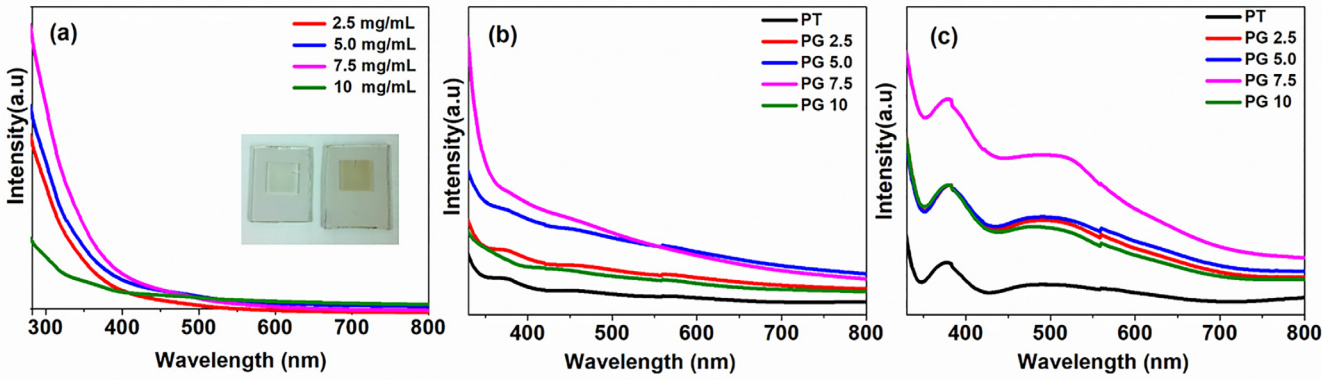

Fig. 4. Absorption spectra of (a) GQDs solution at different concentration at 290 nm peak, with inlet picture of photoelectrodes of pristine TiO_2 (left side) and TiO_2–GQDs (right side). (b) Pristine TiO_2 (PT) and TiO_2-GQDs of PG 2.5, 5.0.7.5 and 10 films (b) After immersing in GQDs (c) After GQDs and N719 dye-sensitized.

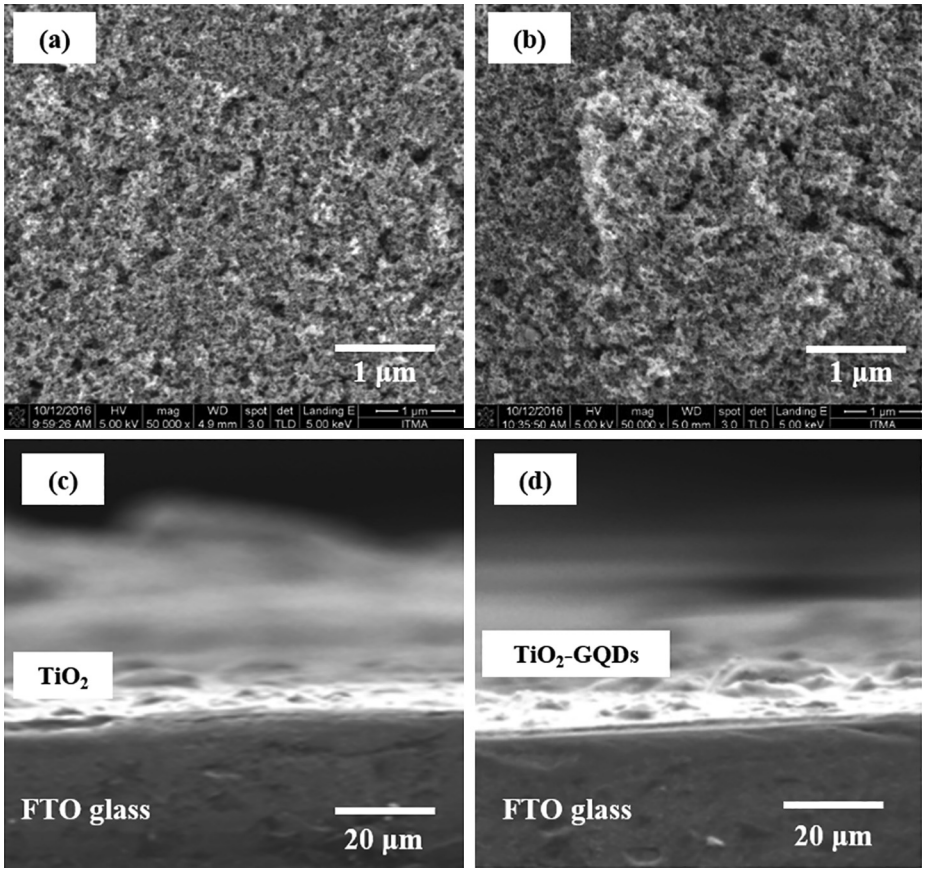

Fig. 5. Surface image of (a) pristine TiO_2 and (b) TiO_2-GQDs films after sensitized GQDs. Cross-sectional image of (c) pristine TiO_2 and (d) TiO_2-GQDs films.

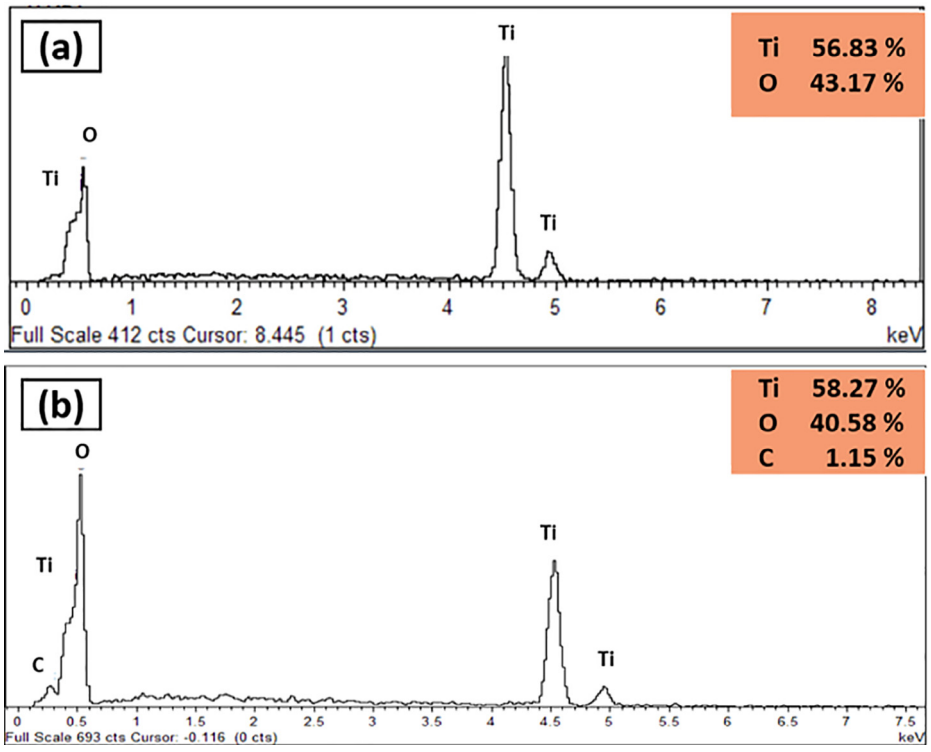

Fig. 6. (a) EDX spectra of PT consist of wt% of Titanium (Ti) and oxygen (O) and (b) PG 7.5 film consist of wt % of Titanium (Ti), oxygen (O) and carbon (C).

Table 1
Photovoltaic parameters of pristine TiO_2 and GQD-TiO_2 photoelectrodes of DSSCs at different concentration.

Cell	Jsc (mA/cm^2)	Voc (v)	FF	ɳ (%)
PT	12.10	0.75	0.45	4.08
PG 2.5	11.14	0.75	0.62	5.15
PG 5.0	11.36	0.75	0.66	5.65
PG 7.5	15.49	0.75	0.60	6.97
PG 10	14.05	0.75	0.45	4.75

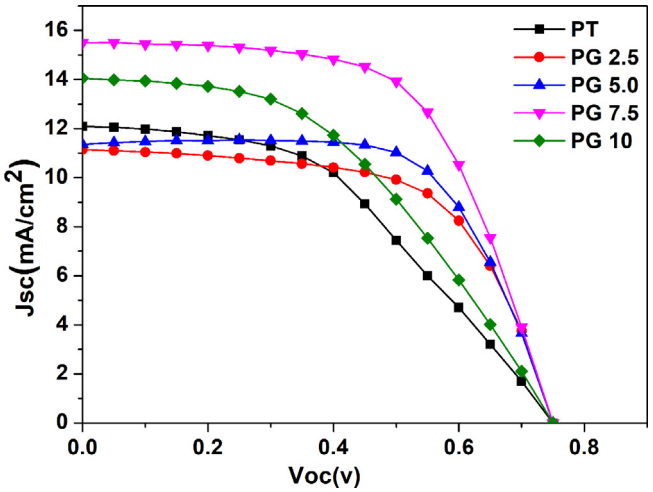

Fig. 7. J-V curves of pristine TiO_2 and TiO_2-GQD photoelectrodes of DSSC.

Electrochemical characteristic

The electrochemical behavior of TiO_2-GQDs photoelectrodes and pristine TiO_2 were recorded using EIS in the frequency range of 0.01 Hz to 100 kHz. The EIS measurement were shown as in Figs. 8 and 9 with their corresponding impedance values are represented in Table 2. Normally, there are three semicircle in typical Nyquist plot. Series resistance, Rs in the equivalent circuit represented the initial value of semicircle intercept at real-axis. Rct1 in the equivalent circuit represent semicircle at higher frequency belongs to the charge transfer resistance at the platinum electrode and electrolyte interface while the the impedance Z_{02} consists of charge transfer resistance, R_{ct2} between the TiO_2/dye/electrolyte interfaces represented by second semicircle at the

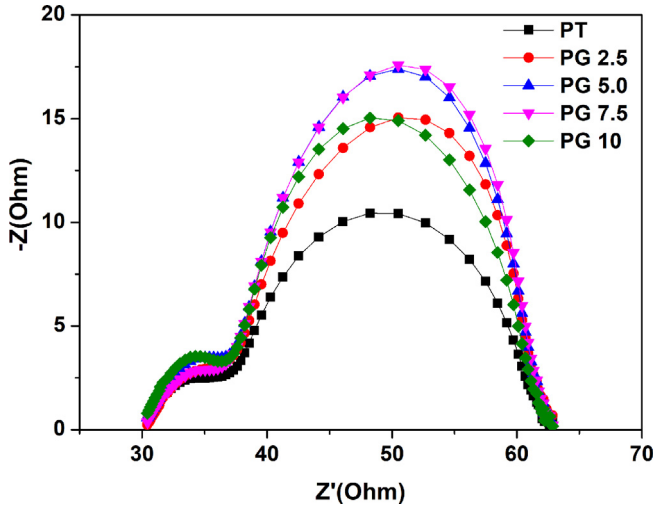

Fig. 8. Nyquist plots with modified photoelectrodes of PG 2.5, PG 5.0, PG 7.5, PG 10 and PT of DSSCs.

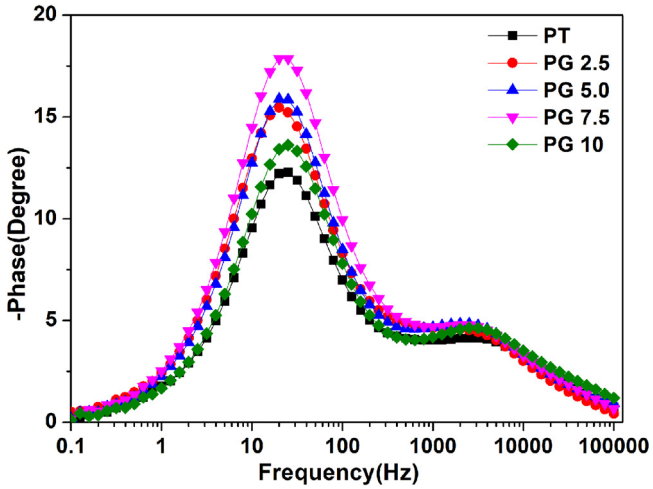

Fig. 9. Bode plot with modified photoelectrodes of PG 2.5, PG 5.0, PG 7.5, PG 10 and PT of DSSCs.

Table 2
EIS parameter values for pristine TiO_2 (PT) and TiO_2-GQD of PG 2.5, PG 5.0, PG 7.5, PG 10 cells.

	Rs (Ω)	R_{ct2} (Ω)	$\omega_{max\ (Hz)}$	Ʈs (ms)	Cu (mF)	Ʈn (ms)	ɳc (%)
PT	30.17	24.30	25.12	7.66	0.21	4.95	39.28
PG2.5	31.96	35.41	19.95	6.51	0.17	5.87	47.39
PG5.0	35.23	39.73	19.95	6.71	0.15	6.09	47.59
PG7.5	29.80	41.98	19.95	5.52	0.15	6.33	53.42
PG10	37.57	34.20	19.95	7.61	0.16	5.66	42.64

middle frequency range. Fig. 8 showns the Nyquist plot of TiO_2 phoelectrode of DSSC with different concentration of GQDs solution. In this study, the FTO Rs of 15 Ω was not considered. The lowest Rs of 36.60 Ω was generated by cell of PG 7.5 compare to PT cell of 37.16 Ω. This was due to improvement of conductivity by GQDs on photoelectrode which function as linkage and rapidly capture electrons and transport them to the other TiO_2 particle [33,34]. Thus PG 7.5 cell generated shortest transport time at 5.52 ms compare to other cell.

The Rct2 is increased as the GQDs content getting higher, this consistent with current density, Jsc generated by PG 7.5. Cell with 7.5 mg/ml GQDs generated maximum Jsc and Rct2 at 15.49 mA/cm^2 and 41.95 Ω. When the charges moves to the TiO_2/electrolytes interfaces, subsequently it cause charge recombination within electrolyte, I_3 and dye was oxidized rapidly. This generating dark current in the cell and affecting the photon to current conversion efficiency, ɳ. Hence, a large charge transfer resistance, R_{ct2} is vital for reducing dark current from charge recombination and generating higher Jsc for DSSC [38].

In DSSC, the charge transport behavior explained by the electron lifetime $Ʈ_n$. The ω_{max} in the bode plot as in Fig. 9 of cell of PT and PG 7.5 at 32.12 Hz and 25.12 Hz respectively. Since the relationship of electron lifetime is inversely proportional to ω_{max} as written in Eq. (1). The highest $Ʈ_n$ generated at 6.33 ms under optimum concentration GQD of 7.5 mg/ml. Electrons with longest $Ʈ_n$ proved it suppressed recombination phenomenon, as suggested by highest Rct [39]. Table 2 shown the best cell namely PG7.5 with lowest Rs, highest Rct, longer $Ʈ_n$ and highest charge collection efficiency (CCE) of 53.42%. The CCE value for all modified TiO_2-GQD photoelectrodes were higher compared to pristine TiO_2 cells due to suppression of recombination electron in the DSSC. The impedance parameters of DSSC were fitted by the equivalent circuit consists of Rs, impedance Z_{01}(Rct1 and Cpe1) and Z_{02} (Rct2 and Cpe2) as shown in Fig. 10. The photovoltaic performance of our cells are validated with EIS result, since cell of PG 7.5 also produced highest Jsc and ɳ compare to PT cell.

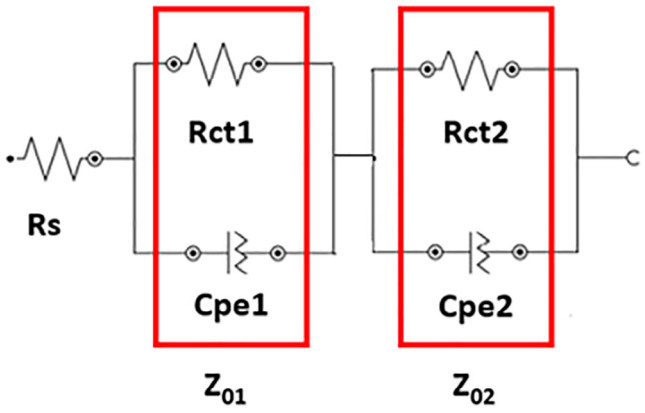

Fig. 10. The impedance represent by equivalent circuit consist of Rs, Rct1 and Rct2 and Cpe of DSSC.

Conclusion

As summary, GQD from agrowaste biochar was successfully synthesis with desire physical and optical properties by hydrothermal method. The current–density, Jsc and photon-to-current conversion efficiency, ɳ of PG 7.5 cell generated best performance at 15.49 mA cm-^{2} and 6.97% respectively compare to pristine TiO_2 DSSC at 12.10 mA cm^{-2} and 4.08%. The enhancement may due to GQD improved light absorption intensity and PL property own by GQD which generated more electron-hole pairs in the solar cell. Thus, enhance the photovoltaic parameters of Jsc and ɳ of DSSC. The fill factors generated for all TiO_2-GQDs cells were higher compare to pristine TiO_2 cell with average of ~0.63. However, PG 10 fill factor generated at 0.45 maybe due to agglomeration of GQD onto photoelectrode. Similarly, for EIS study, cell PG 7.5 also shown higher charge collection efficiency of 53.42%, an improvement of ~35.99% compare to pristine TiO_2 cell. This behavior was due to the highest τ_n generated at 6.33 ms under optimum concentration of GQDs of 7.5 mg/ml. Electrons with longest τ_n proved it supressed recombination phenomenon, as suggested by highest Rct. The EIS and PV performance confirmed that a GQD concentration of 7.5 mg/ml can enhance and optimize Jsc, PCE and charge collection efficiency of DSSC.

Acknowledgement

This research work was supported by Universiti Putra Malaysia grant (PUTRA IPB/2016/9515402).

References

[1] Gong J, Liang J, Sumathy K. Review on dye-sensitized solar cells (DSSCs): fundamental concepts and novel materials. Renew Sustain Energy Rev 2012;16(8):5848–60.
[2] Papageorgiou Nik. Dye-sensitized solar cells rival conventional cell efficiency. Mediacom 2013 [Online]. Available: https://actu.epfl.ch/news/dye-sensitized-solar-cells-rival-conventional-ce-2/.
[3] Kumari JMKW, Senadeera GKR, Dissanayake MAKL, Thotawatthage CA. Dependence of photovoltaic parameters on the size of cations adsorbed by TiO2 photoanode in dye-sensitized solar cells. Ionics (Kiel) 2017:1–6.
[4] Tripathi M, Chawla P. CeO2-TiO2 photoanode for solid state natural dye-sensitized solar cell. Ionics (Kiel) Feb. 2015;21(2):541–6.
[5] Park J, Viscardi G, Barolo C, Barbero N. Near-infrared sensitization in dye-sensitized solar cells. Chim Int J Chem 2013;67(3):129–35.
[6] Sarker AK, Kang MG, Hong J-D. A near-infrared dye for dye-sensitized solar cell: catecholate-functionalized zinc phthalocyanine. Dye Pigm 2012;92(3):1160–5.
[7] Hao S, Shang Y, li D, Agren H, Yang C, Chen G. Enhancing dye-sensitized solar cell efficiency through broadband near-infrared upconverting nanoparticles. Nanoscale 2017;9.
[8] Nadia SR, Khanmirzaei MH, Ramesh S, Ramesh K. Quasi-solid-state agar-based polymer electrolytes for dye-sensitized solar cell applications using imidazolium-based ionic liquid. Ionics (Kiel) 2017;23(6):1585–90.
[9] Roy-Mayhew JD, Bozym DJ, Punckt C, Aksay IA. Functionalized graphene as a catalytic counter electrode in dye-sensitized solar cells. ACS Nano Oct. 2010;4(10):6203–11.
[10] Zhang DW, et al. Graphene-based counter electrode for dye-sensitized solar cells. Carbon N Y 2011;49(15):5382–8.
[11] Liu Q, Li Z-S, Chen S-L. Metal-embedded graphene as potential counter electrode for dye-sensitized solar cell. Ind Eng Chem Res Jan. 2016;55(2):455–62.
[12] Ribeiro F, Maçaira J, Cruz R, Gabriel J, Andrade L, Mendes A. Laser assisted glass frit sealing of dye-sensitized solar cells. Sol Energy Mater Sol Cells 2012;96(Supplement C):43–9.
[13] Lim SP, et al. Gold–silver@TiO 2 nanocomposite-modified plasmonic photoanodes for higher efficiency dye-sensitized solar cells. Phys Chem Chem Phys Jan. 2017;19(2):1395–407.
[14] Samaila B, Jafaar Haslina, Khalifa Ali, Shafie Suhaidi, Rashid Suraya Abdul. Process parameters on the efficiency N-TiO2 dye sensitised solar cell using response surface methodology (RSM) Buda. Sci Technol 2017;25:111–8.
[15] Sudhagar P, et al. Exploring graphene quantum dots/TiO2 interface in photoelectrochemical reactions: solar to fuel conversion. Electrochim Acta 2016;187:249–55.
[16] Wei L, et al. Enhanced performance of dye sensitized solar cells by using a reduced graphene oxide/TiO2 blocking layer in the photoanode. Thin Solid Films 2017;639:12–21.
[17] Zhang X, Liu F, Huang Q-L, Zhou G, Wang Z-S. Dye-sensitized W-doped TiO2 solar cells with a tunable conduction band and suppressed charge recombination. J Phys Chem C Jun. 2011;115(25):12665–71.
[18] Momina Khannam SKD, Sharma Shyamalima, Dolui Swapnil. A graphene oxide incorporated TiO2 photoanode for high efficiency quasi solid state dye sensitized solar cells based on a poly-vinyl alcohol gel electrolyte. J RSC Adv 2016;6:55406–14.
[19] Batmunkh M, Dadkhah M, Shearer CJ, Biggs MJ, Shapter JG. Incorporation of graphene into SnO2 photoanodes for dye-sensitized solar cells. Appl Surf Sci 2016;387(Supplement C):690–7.
[20] Guo X, Lu G, Chen J. Graphene-based materials for photoanodes in dye-sensitized solar cells. Front Energy Res 2015;3:50.
[21] Kim S-B, et al. Effects of graphene in dye-sensitized solar cells based on nitrogen-doped TiO2 composite. J Phys Chem C Jul. 2015;119(29):16552–9.
[22] Long R. Understanding the electronic structures of graphene quantum dot physisorption and chemisorption onto the TiO2 (110) surface: a first-principles calculation. ChemPhysChem 2013;14(3):579–82.
[23] Wang T-H, Huang T-W, Tsai Y-C, Chang Y-W, Liao C-S. A photoluminescent layer for improving the performance of dye-sensitized solar cells. Chem Commun 2015;51(33):7253–6.
[24] Chinnusamy Jayanthi S, Kaur R, Erogbogbo F. Graphene quantum dot – Titania nanoparticle composite for photocatalytic water splitting. MRS Adv 2016;1(28):2071–7.
[25] Fang X, et al. Graphene quantum dots optimization of dye-sensitized solar cells. Electrochim Acta 2014;137:634–8.
[26] Qu D, et al. Highly luminescent S, N co-doped graphene quantum dots with broad visible absorption bands for visible light photocatalysts. Nanoscale 2013;5(24):12272.
[27] Mihalache I, et al. Charge and energy transfer interplay in hybrid sensitized solar cells mediated by graphene quantum dots. Electrochim Acta 2015;153:306–15.
[28] Razbirin BS, Rozhkova NN, Sheka EF, Nelson DK, Starukhin AN. Fractals of graphene quantum dots in photoluminescence of shungite. J Exp Theor Phys 2014;118(5):735–46.
[29] Ma C-B, et al. A general solid-state synthesis of chemically-doped fluorescent graphene quantum dots for bioimaging and optoelectronic applications. Nanoscale 2015;7(22):10162–9.
[30] Wang S, Cole IS, Li Q. Quantum-confined bandgap narrowing of TiO2 nanoparticles by graphene quantum dots for visible-light-driven applications. Chem Commun 2016;52(59):9208–11.
[31] Li Y, et al. Electrochimica acta graphite with different structures as catalysts for counter electrodes in dye-sensitized solar cells $. Electrochim Acta 2015;179:211–9.
[32] Lee E, Ryu J, Jang J. Fabrication of graphene quantum dots via size-selective precipitation and their application in upconversion-based DSSCs 1. Experimental section. Chem Commun 2013;49:9995.
[33] Peng J, et al. Graphene quantum dots derived from carbon fibers. Nano Energy 2012;2(12):844–9.
[34] Gupta BK, Kedawat G, Agrawal Y, Kumar P, Dwivedi J, Dhawan SK. A novel strategy to enhance ultraviolet light driven photocatalysis from graphene quantum dots infilled TiO2 nanotube arrays. RSC Adv 2015;5(14):10623–31.
[36] Fang X, et al. Graphene-compositing optimization of the properties of dye-sensitized solar cells. Sol Energy 2014;101:176–81.
[38] Adachi M, Sakamoto M, Jiu J, Ogata Y, Isoda S. Determination of parameters of electron transport in dye-sensitized solar cells using electrochemical impedance spectroscopy. J Phys Chem B 2006;110(28):13872–80.
[39] Lim SP, Pandikumar A, Lim HN, Ramaraj R, Huang NM. Boosting photovoltaic performance of dye-sensitized solar cells using silver nanoparticle-decorated N, S-Co-doped-TiO2 photoanode. Sci Rep 2015;5(1):11922.